Journal of Engineering Science and Technology
Vol. 13, No. 11 (2018) 3781 - 3794

EFFECT OF STRENGTHENING METHOD AND DEVELOPMENT LENGTH ON FLEXURAL STRENGTH OF RC BEAMS WITH STEEL PLATES

RENDY THAMRIN

Department of Civil Engineering, Faculty of Engineering, Andalas University,
Padang, 25163, West Sumatera, Indonesia
Email: rendy@ft.unand.ac.id

Abstract

The test result of an experimental study on the flexural strength of reinforced concrete beams strengthened with steel plates is presented. The beams were simply supported and loaded monotonically with two point loads. The test variables used in this study were strengthening method and development length of steel plates. Nine beams without strengthening and nine beams strengthened with steel plates were tested until the beams reach the flexural failure specified by crushing of concrete on the top surface of compression region. The test results show that steel plates increase the capacity of the beam significantly and slightly increase the flexural stiffness of the beams. In addition, the ultimate load of the strengthened beams with debonding failure was similar to the beams without strengthening if the load kept increasing until flexural failure. The test results also showed that the debonding failure occurred after the steel plate reach the yield stress value and the development length affects the failure mode of the strengthened beams. Analytical study based on a theoretical moment-curvature calculation of reinforced concrete cross-section was carried out in order to obtain the complete flexural response of the beams analytically. The comparison shows that analytical prediction provides good accuracy for both reinforced concrete beams with and without strengthening.

Keywords: Debonding failure, Development length, Flexural strength, Steel plate, Strengthening.

1. Introduction

Improving the members of reinforced concrete structures by using epoxy resins [1] and steel bars or plates adhesively attached to the tension face of concrete has been used for the past three decades [2-10]. This method is a simple and low-cost method of flexural strengthening.

As reported by Swamy et al. [2], reinforced concrete beams strengthened with externally glued steel plates show higher flexural strength and rigidity compared to beams without strengthening. As reported by Oehlers et al. [4], however, reinforced concrete members strengthened with steel plates can fail suddenly due to the separation of the plates and concrete surfaces. Therefore, structural members that use externally glued steel plates must be designed to avoid this sudden failure.

A previous study designed to observe the contribution of steel plates on the flexural strength of the strengthened beams has been carried out [8]. In this past study, steel plates were glued to the soffits of the beams using near surface mounted method. Debonding failure after yielding of the steel plates with concrete cover separation occurred on two of the strengthened beams. The result also showed that the strengthened beam has higher flexural strength.

Although reinforced concrete beam strengthening with steel plates has been extensively researched, there are still some important issues, such as debonding problem, that need to be investigated. The main purpose of this study is to examine the effect of strengthening method (tension face plated and near-surface mounting) and development length of steel plates on flexural strength of strengthened reinforced concrete beams experimentally.

Analytical prediction using theoretical moment-curvature determination of reinforced concrete cross section was also carried out and a computer program was developed. The output of the program is the flexural response of the beam cross-section in the form of a load-deflection curve. Analytical results then compared with the data obtained from the test.

2. Experimental Study

A series of experimental studies were carried out on simply supported reinforced concrete beams strengthened with steel plates. Eighteen reinforced concrete beams were divided into three groups with six teams in each group. Each group consisted of three beams as control specimens and three beams flexural strengthened with steel plates. The complete list of material properties used in this study is shown in Table 1. Group II was adopted from author's test data in a previous study [8].

Fresh concrete was supplied by the ready-mix concrete company. The cylindrical specimens were taken out from a concrete mixer truck before the concrete poured into the beams framework. The maximum aggregate size of concrete was 10 mm and the concrete compressive strength at age 28 days for each group are listed in Table 1. The concrete compressive strength was obtained from the standard test method for compressive strength of cylindrical specimens with 150 mm diameter of cross-section and 300 mm high (ASTM C39/C39M-14) [11]. The compressive testing machine used for concrete compression test is shown in Fig. 1(a).

Longitudinal reinforcement used was deformed steel bars with 13 mm diameter of cross-section. Three ratios of longitudinal reinforcement used for control specimens and for both types of strengthening method were 1%, 1.5% and 2.5%. All beams were reinforced with 10 mm diameter closed type stirrups and the spacing between stirrups was 100 mm. The tensile strength of steel bars and steel plates was obtained from a standard test method for the tensile strength of steel products (ASTM A370-16) [12]. Figure 1(b) shows the universal testing machine used for the tensile test of steel bars and steel plates. The results of the tensile test in term of yielding strength are listed in Table 1.

Table 1. Material properties.

Group	Concrete compressive strength, *fc* (MPa)	Yield strength, *fy* (MPa)		
		Longitudinal reinforcement	Transversal reinforcement	Steel plate
I	27.0	417	368	240
II	23.0	580	391	250
III	23.7	340	389	304

(a) Concrete compression test.

(b) Universal testing machine used for tensile test of steel bar.

Fig. 1. Equipment used for material test.

Figure 2 illustrates the side view and cross-section of control beams and reinforced concrete beams strengthened with steel plates used in this study. The cross-sections of the beams were 125 mm wide and 250 mm high. The sheer span length was 800 mm, the length of constant moment zone was 400 mm and the total length for all beams was 2300 mm. To avoid bond failure in support region the sufficient development length of longitudinal reinforcement beyond the support was used as 150 mm as suggested in references [13-15]. The position of loads and the dimension of the beams are shown in Fig. 2(a).

Three methods of mounting the steel plates on the soffit of the beam can be seen in Figs. 2(b) to (d). In the case of beams labelled BP0 the surface of the steel plates was directly bonded with an adhesive (epoxy) to the tension face of the beams after removing dust and fine particles from the bottom surface of the beams (tension face plated). Epoxy used in this study is Sikadur 31 with a tensile adhesion strength of 12 MPa after 3 days of curing time. This epoxy can be used to glue steel on concrete and the price of this epoxy is not too expensive. The cross-section detail of beam BP0 showing the position of the steel plate is illustrated in Fig. 2(e).

The effect of development length (*Lp*) of near surface mounted steel plate was observed in beams BP and BP2. In these beams (BP and BP2), the groove cuts were initially arranged before pouring fresh concrete into the formwork of the beam. After curing the concrete beams for 28 days formwork is released. Then, the groove surfaces were cleaned by compressed air to take out fine particles and dust. The epoxy adhesive is filled halfway into the grooves using a palette knife before inserting the steel plates. The steel plates (3 mm thick and 50 mm width) were immediately placed inside the grooves and pressed lightly along the plate to the adhesive. The grooves were finally filled with epoxy adhesive paste and the surface was levelled as illustrated in Fig 2(f). Support condition for beam BP2 beams is illustrated in Fig. 2(g).

The hydraulic jack with 500 kN capacity was used to applied two-point loads monotonically until failure. The magnitude of the applied load was measured using a load cell placed above the steel spreader beam as shown in Fig. 3(a). Three linear variable displacement transducers (LVDT's) were used to measure the deflections at mid-span and at both loading points. Load cell and LVDT's were connected to a data logger. The cracks occurred during the test were observed and the crack loads value were plotted beside the crack line. To ensure the beams reached the ultimate state, the loading was stopped due to crushing of concrete on the top surface of the compression region as shown in Fig. 3(b).

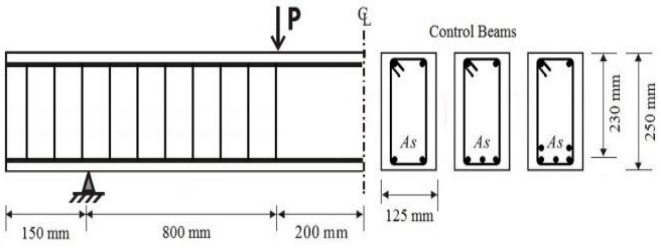

(a) Control beams.

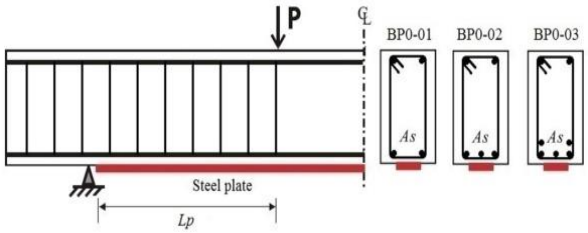

(b) BP0 (tension face plated).

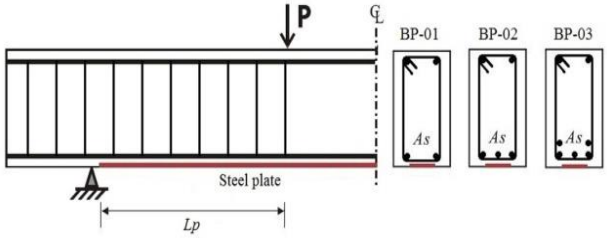

(c) BP (near surface mounted).

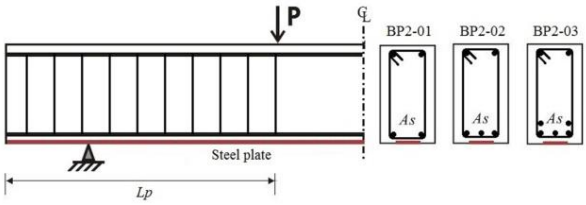

(d) BP2 (near surface mounted).

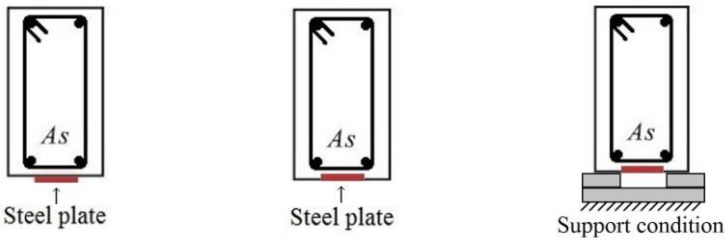

(e) Cross section detail of BP0 beams. **(f) Cross section detail of BP and BP2 beams.** **(g) Support condition for BP2 beams only.**

Fig. 2. Type of beam specimens and cross-section detail of each group.

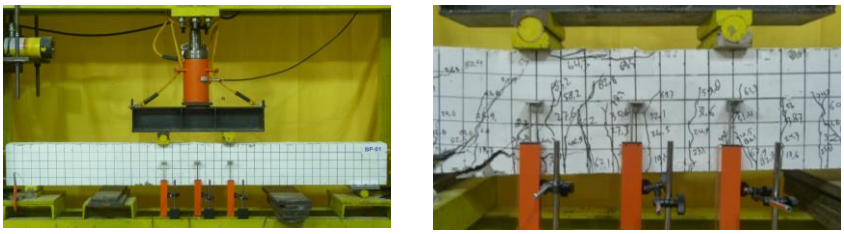

(a) Beam before test (test setup). **(b) Typical failure after test.**

Fig. 3. Experimental setup.

3. Analytical Study

According to Thamrin [8] and Park and Paulay [16], a numerical study based on the theoretical moment-curvature calculation of reinforced concrete cross section used in references was applied in this study. The first step of this method is performed by dividing the cross section into a finite number of reinforcement and concrete layers as illustrated in Fig. 4. In the analytical model, the steel plate is assumed as the reinforcement layer and connection between reinforcement layers and concrete layers are assumed to be perfectly bond. Hence, the strain distribution along the height of the beam cross-section can be assumed to be linear as shown in Fig. 4.

The strain, ε_i, in the concrete and reinforcement elements for an assumed value of curvature, φ, and the lever arm of each element, y_i, can be calculated as:

$$\varepsilon_i = \varepsilon_o - (\varphi\, y_i) \tag{1}$$

The second step is calculating the stresses by using a given stress-strain law of concrete and steel. The stresses, σ_i, acting on each reinforcement layers, concrete elements and the steel plate can be determined as:

$$\sigma_i = f(\varepsilon_i) \tag{2}$$

As suggested by Mander et al. [17], the stress-strain law of concrete in compression applied in this study is adopted from the model, while for concrete in tension a linear model up to the maximum concrete tensile strength without a tension stiffening effect is used. The stress-strain law for steel bars and steel plates used in this study is a bi-linear model.

The third step is calculating the internal forces, F_i, for each of the concrete elements and reinforcement layers with an area, A_i, can be obtained as:

$$F_i = A_i \, \sigma_i \tag{3}$$

The fourth step is checking whether the equilibrium of internal forces is satisfied. An iterative procedure is required to obtain the value of axial strain, ε_o, which fulfilled the equilibrium of the internal forces. The fifth step is calculating the internal moment, M, in the cross-section as:

$$M = \sum F_i y_i \tag{4}$$

The last step is to calculate the load, P, and deflection, δ, values by using the appropriate moment and curvature distribution with each incremental step along the length, L, of the beam and can be calculated as:

$$\delta = \int_0^{L/2} x \varphi dx \tag{5}$$

The complete details of the computation procedure can be found in the literature [8, 16]. The algorithm of the computation procedure is illustrated in Fig. 5. The calculation process was aided by a computer program (using FORTRAN programming language) developed by the author.

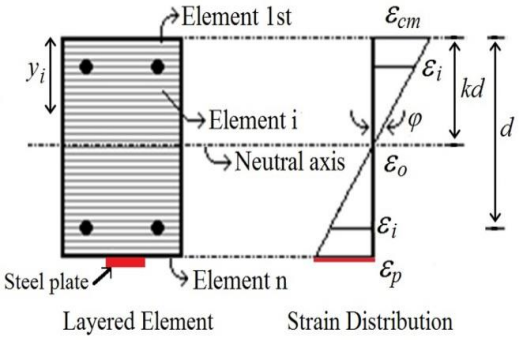

Fig. 4. Analytical model and strain distribution along the height of beam cross section.

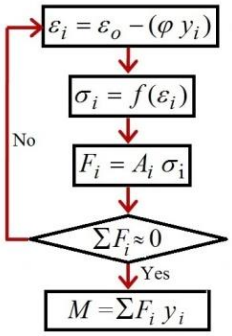

Fig. 5. The algorithm of the computation procedure [8, 9].

4. Results and Discussion

Table 2 shows beam data, the calculated beam capacities and the test results. Where ϕ_b is the diameter of longitudinal reinforcement, N is a number of tensile longitudinal reinforcement, ρ is the ratio of longitudinal reinforcement, ϕ_s is the diameter of stirrups, s is spacing of stirrups, t is plate thickness and w is the plate width.

Table 2. Beam data, failure modes and test results.

Specimen		Longitudinal reinforcement (tensile)			Stirrups		Steel plate		Calculated flexural capacity	Experimental			Failure mode
		ϕ_b (mm)	N	ρ (%)	ϕ_s (mm)	s (mm)	t (mm)	w (mm)	Vf (kN)	First crack (kN)	Deb. load (kN)	Max. load (kN)	
Group I	**BC0-01**	13	2	1.0	10	100	Control specimens		25	11.0	-	29	F
	BC0-02		3	1.5					37	12.0	-	39	F
	BC0-03		5	2.5					54	10.5	-	53	F
	BP0-01		2	1.0			3	50	35	11.0	-	38	F
	BP0-02		3	1.5					46	10.0	26.2	39	F
	BP0-03		5	2.5					66	10.5	38.4	54	F
Group II [8]	**BC-01**		2	1.0			Control specimens		35	8.9	-	39	F
	BC-02		3	1.5					51	8.5	-	52	F
	BC-03		5	2.5					76	6.0	-	71	F
	BP-01		2	1.0			3	50	44	8.8	42.0	42	F
	BP-02		3	1.5					60	9.3	-	59	F
	BP-03		5	2.5					81	12.4	79	79	F
Group III	**BC2-01**		2	1.0			Control specimens		22	4.9	-	23	F
	BC2-02		3	1.5					32	5.3	-	38	F
	BC2-03		5	2.5					48	5.1	-	51	F
	BP2-01		2	1.0			3	50	35	5.7	-	38	F
	BP2-02		3	1.5					45	6.8	-	51	F
	BP2-03		5	2.5					63	5.1	-	64	F

Representative crack patterns of the beams at failure are shown in Fig. 6. For all control beams, the flexural crack was first initially developed in the zone between the two-point loads (constant moment zone) at an average load level of 8.4 kN. Higher values of the first crack load were observed in beams with steel plates showing the contribution of steel plates to withstand tensile forces. The diagonal shear cracks develop in the shear span zone after the occurrence of flexural cracks in the tension side of the beams as shown in Fig. 6.

In this study, debonding failure occurred after the occurrence of diagonal shear cracks. The yielding points of tensile reinforcement occurred at various load stages depending on the amount of the tensile longitudinal reinforcement. Finally, all the beams failed in flexural failure as indicated by higher values of deflection and crushing of concrete on the top fibre of the compression zone.

The modes of failure for each beam are listed in Table 2. Two types of failure mode were observed, i.e., debonding failure (*D*) indicated by debonding from plate end and debonding failure with concrete cover separation and flexural failure (*F*) indicated by crushing of concrete on the top of compression zone, yielding of steel plate and yielding of tensile longitudinal reinforcement as shown in Fig. 7. In this experimental study, if a debonding failure occurred, load continued to be increased until flexural failure occurred, and the beams reached the ultimate condition as shown in Fig. 7. The maximum loads listed in Table 2 are the load of flexural failure. The values of debonding load are listed in Table 2 and pointed out in load-deflection curves in Fig. 7.

The first mode of failure (debonding) was observed in two beams from Group I (BP0-02 and BP0-03) and two beams from Group II (BP-01 and BP-03) while only the second mode of failure (flexural) was observed from beams in Group III. This difference was caused by the different mounting methods of the steel plates. Additionally, due to longer development length of the steel plates, no debonding failure was found on the strengthened beams in Group III.

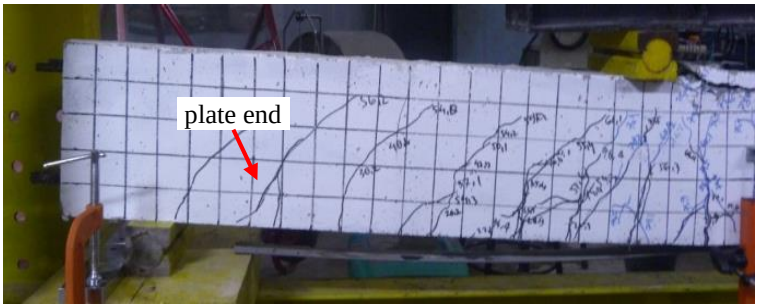

(a) BP0-02.

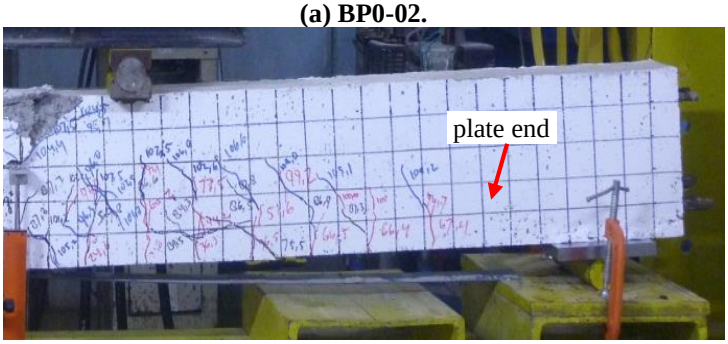

(b) BP0-03.

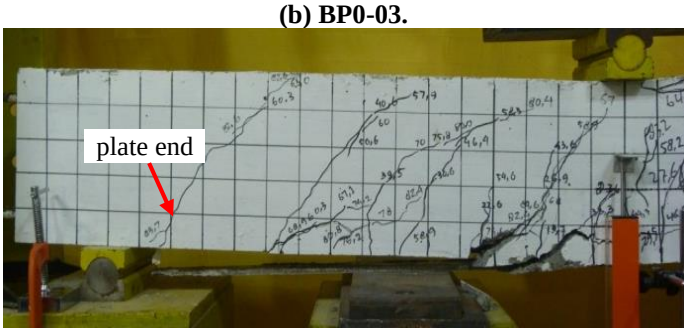

(c) BP-01.

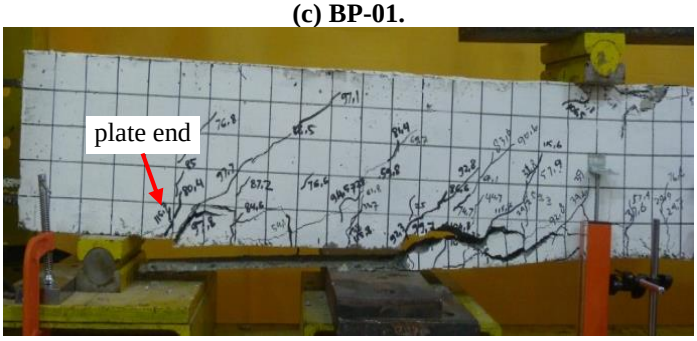

(d) BP-03.

Fig. 6. Debonding from plate end (BP0-02 and BP0-03) and debonding failure with concrete cover separation (BP-01 and BP-03).

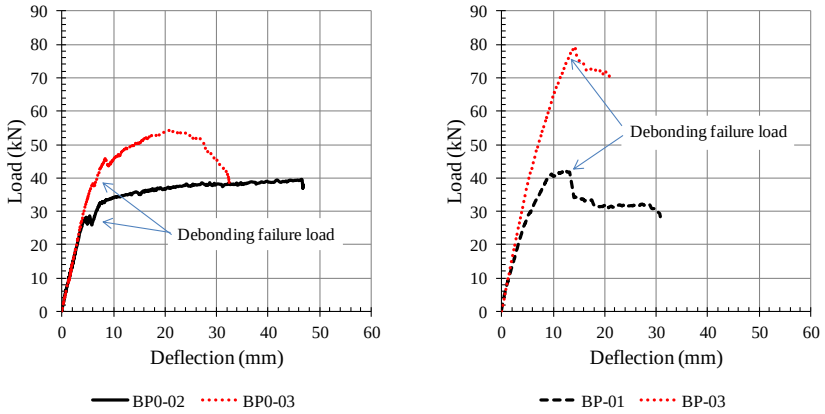

(a) Group I. **(b) Group II.**

Fig. 7. Load-deflection curves of beams with debonding failure.

In order to observe the effect of tensile reinforcement ratio on the beam capacity, the midpoint deflections obtained from the test are plotted against the point loads as shown in Fig. 8 (black line). It is shown that the tensile reinforcement ratio significantly affected the beam capacity for all beams, both with and without steel plates. However, an increase in the tensile reinforcement ratio led to an increase in the shear forces sustained before failure. Hence, the possibility of debonding failure for beams with higher reinforcement ration is higher when beams are strengthened with steel plates.

A comparison between analytical (red line) and experimental (black line) load-deflection curves are shown in Fig. 8 (a to f). The analytical model can accurately predict the full flexural response of all beams. The analytical result indicates that the flexural strength of the plated beams is higher than for beams without steel plates by 6 to 60%, depending on the values of concrete compression strength, the ratio of longitudinal reinforcement, the yield strength of longitudinal reinforcement and the yield strength of steel plates. In addition, the test results obtained from the analytical study indicate that debonding failure for BP0-02, BP0-03, BP-01, and BP-03 occurs after yielding of the steel plates.

The debonding failure loads of beams BP0-02, BP0-03, BP-01 and BP-03 are also shown in Fig. 8(b) and (d). The failure load for beams BP0-02 and BP0-03 was similar to that beams without steel plates (BC0-02 and BC0-03) as shown in Fig. 8(b). In this case, the debonding failure occurred before yielding of the tensile reinforcement. However, in beams, BP-01 and BP-03 debonding failure occurred after yielding of the tensile reinforcement. The resulting increase in capacity can be seen in Fig. 8(d). In addition, it is observed from this study that the occurrence of debonding failure can be avoided by increasing the development length (Lp) of the steel plates. The flexural strength of control and strengthened beams for Group III can be seen in Figs. 8(e) and (f).

Figure 9 shows the comparison of load-deflection curves between beams with (red line) and without (black line) steel plates. In the case of beams with steel plates, only beam BP0-01 in Group I and beam BP-02 in Group II reached the flexural capacity without premature debonding failure. The flexural capacities of the

strengthened beams in Group I and Group II were about 31% and 13% higher than that of the control beams.

It is also shown in Fig. 9(b) that the flexural capacity of the beams in Group II was relatively high compared to that of beams in Group I and III due to the higher value of yield strength of the tensile reinforcement (580 MPa). This frequently led to debonding failure, which started at the plate ends and developed towards the centre of the beam (debonding failure with concrete cover separation). Figure 9(c) shows that all the beams with steel plates in Group III (BP2-01, BP2-02 and BP2-03) reached flexural capacities that were 65%, 33%, and 25% higher than the control beams. It also shows that steel plates increased the stiffness of all the strengthened beams significantly.

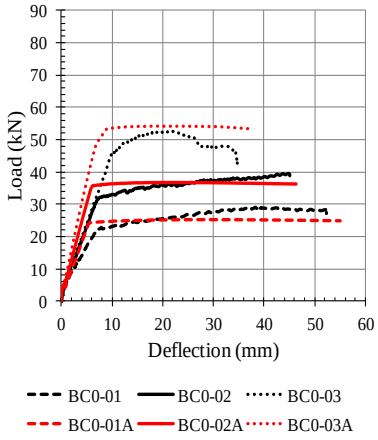

(a) Group I (control beams).

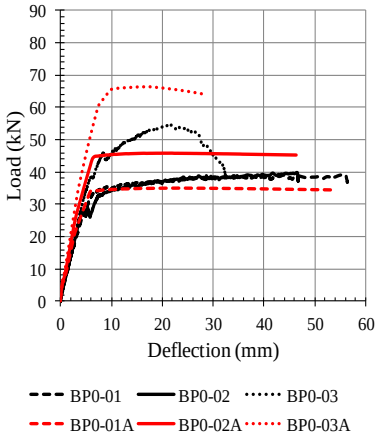

(b) Group I (with steel plates).

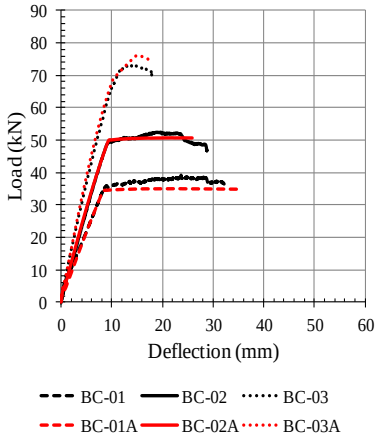

(c) Group II (control beams).

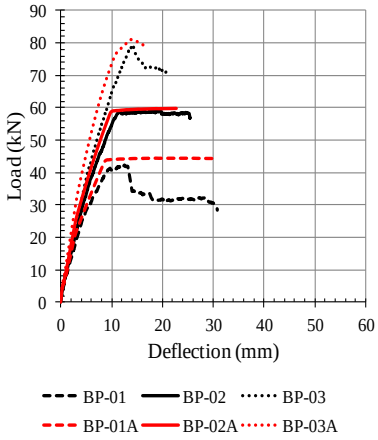

(d) Group II (with steel plates).

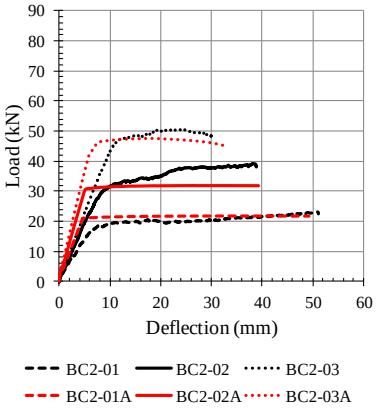

(e) Group III (control beams).

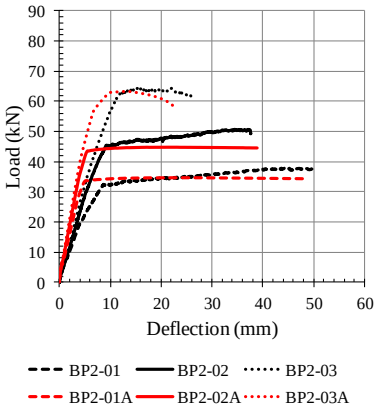

(f) Group III (with steel plates).

Fig. 8. Comparison between analytical prediction and test result.

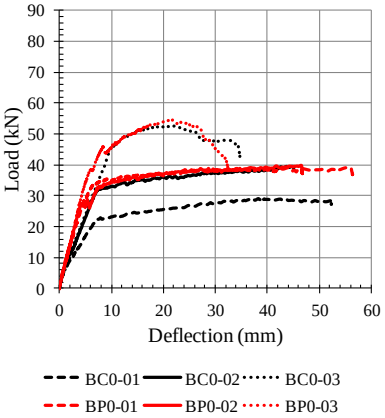

(a) Group I.

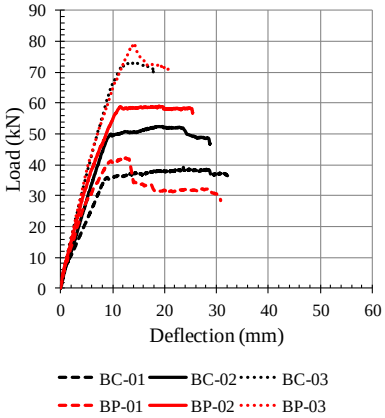

(b) Group II.

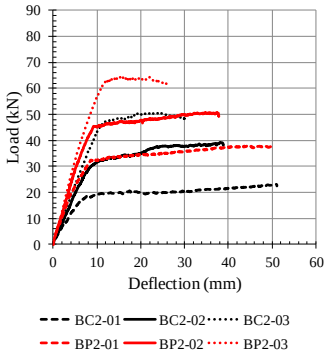

(c) Group III.

Fig. 9. Comparison between beams with and without steel plates.

In order to compare the experimental debonding load with the available theoretical procedure the value of the ultimate peeling moment is then calculated using Eq. (10):

$$M_{up} = \frac{(EI)_{cp}\ f_b}{0.9\,E_S\,t} \tag{6}$$

where $(EI)_{cp}$ is the flexural rigidity of the cracked plated section, f_b is the Brazilian tensile strength taken as $0.5(f_c')^{0.5}$, E_s is Young's modulus of steel plate and t is the thickness of the steel plate.

Furthermore, the theoretical ultimate peeling load can be determined based on the calculated ultimate peeling moment. The comparison between the theoretical ultimate peeling load and test data is listed in Table 3. It is shown that in the case of beams Group I (tension face plated) the predicted values are closed to the test data. However, in the case of beams Group II (near surface mounted) the test data higher than the predicted values. This result indicates that the near surface mounted method bond more effectively the steel plates to the surface of the concrete.

Table 3. Comparison between theoretical ultimate peeling load and test data.

Beams	M_{up} (kNm)	P_{up} (kN)	Experimental debonding load (kN)
BP0-01	24.93	31.17	-
BP0-02	25.64	32.05	26.2
BP0-03	26.02	32.53	38.4
BP-01	20.96	26.20	42.0
BP-02	21.53	26.91	-
BP-03	22.71	28.38	79.0
BP2-01	20.77	25.96	-
BP2-02	20.39	25.49	-
BP2-03	20.83	26.04	-

5. Conclusions

In this paper, two strengthening methods to increase the flexural capacity of reinforced concrete beams are presented. The first method was carried out by glueing directly the steel plates to the tension surface of the beams and the second was by installing the steel plate using near surface mounted method. In the second method, two types of different development length were used in order to examine the effect of plate length in the shear span zone. Eighteen reinforced concrete beams with and without steel plates were tested. The comparison between these two strengthening methods are discussed and based on the test results the following conclusions are drawn:

- The analytical model based on theoretical moment-curvature calculation predicts the full flexural response of beams with and without steel plates accurately.
- The flexural capacity of the beam is significantly influenced by the ratio of tensile reinforcement to both beams with and without steel plate. The flexural capacity of the strengthened beams was 6 to 65% higher than beams without steel plates.
- Load-deflection curves show that flexural stiffness of beams strengthened with steel plates slightly higher than beams without steel plates.
- Failure mode and crack patterns of the beams are significantly affected by the method used for strengthening. Near-surface mounted steel plate method bond more effectively to the surface of the concrete than tension face plated method.

- Two modes of debonding failure of steel plates were observed from the test, the first one is debonding from plate end (BP0-02 and BP0-03) and the second is debonding failure with concrete cover separation (BP-01 and BP-03). However, the test result found that no debonding failure was observed in the beam in Group III.
- The value of theoretical ultimate peeling load obtained using Eq. (6) correlates well with the test result of Group I (tension face plated) but not for Group II (near surface mounted).
- Overall observation from the experimental work found that the method used for strengthening and the development length (*Lp*) applied on the bottom surface of the beams affect the failure mode of the strengthened beams.

Acknowledgement

The author would like to thank Engineering Faculty, Andalas University for the financial support through Hibah Publikasi Fakultas Teknik 2017 with contract number 029/UN.16.09D/PL/2017.

Nomenclatures

A_i	Area of each concrete and reinforcement element
A_s	Area of longitudinal reinforcement
EI_{cp}	The flexural rigidity of the cracked plated section
E_s	Young's modulus of steel plate
f_b	Brazilian tensile strength
f_c'	Concrete compressive strength
f_y	Yield strength of longitudinal reinforcement
F_i	Force in each concrete and reinforcement element
L_p	Development length of the steel plate
M	Total moment of cross-section
M_{up}	Ultimate peeling moment
N	Number of longitudinal reinforcement
P_{up}	Ultimate peeling load
s	Stirrups space
t	Thickness of steel plate
V_f	Calculated flexural strength of concrete
V_m	Maximum load
w	Width of steel plate
y_i	Lever arm of each element

Greek Symbols

δ	Beam deflection calculated from obtained curvature value
ε_t	Strain in each concrete and reinforcement element
ε_o	Strain at the centre of beam cross section
μ	Curvature
ρ	Ratio of longitudinal reinforcement
ϕ_b	Diameter of longitudinal reinforcement
ϕ_s	Diameter of stirrups

Abbreviations

LVDT	Linear Variable Displacement Transducers

References

1. Zaidir; Thamrin, R.; and Dalmantias, E. (2017). Evaluation of the pre-cracked RC beams repaired with sealant injection method. *International Journal on Advanced Science, Engineering and Information Technology*, 7(2), 380-386.
2. Swamy, R.N.; Jones, R.; and Bloxham, J.W. (1989). Structural behaviour of reinforced concrete beams strengthened by epoxy-bonded steel plates. *The Structural Engineer*, 65A(2), 59-68.
3. Swamy, R.N.; Jones, R.; and Charif, A. (1989). The effect of external plate reinforcement on the strengthening of structurally damaged RC beams. *The Structural Engineer*, 67(3), 45-56.
4. Oehlers, D.J.; and Moran, J.P. (1990). Premature failure of externally plated reinforced concrete beams. *Journal of Structural Engineering*, 116(4), 978-995.
5. Oehlers, D.J.; Ali, Mohamed, A.M.S.; and Luo, W. (1998). Upgrading continuous reinforced concrete beams by gluing steel plates to their tension faces. *Journal of Structural Engineering*, 124(3), 224-232.
6. Swamy, R.N.; Mukhopadhyaya, P.; and Lynsdale, C.J. (1999). Strengthening for shear of RC beams by external plate bonding. *The Structural Engineering*, 77(12), 19-30.
7. Altin, S.; Anil, O.; and Kara, M.E. (2005). Improving shear capacity of existing RC beams using external bonding of steel plates. *Engineering Structures*, 27(5), 781-791.
8. Thamrin, R. (2017). Analytical prediction on flexural response of RC Beams strengthened with steel plates. *MATEC Web Conference*, 103, 9 pages.
9. Thamrin, R.; and Sari, R.P. (2017). Flexural capacity of strengthened reinforced concrete beams with web bonded steel plates. *Procedia Engineering*, 171, 1129-1136.
10. Oehlers, D.J. (1992). Reinforced concrete beams with plates glued to their soffits. *Journal of Structural Engineering*, 118(8), 2023-2038.
11. ASTM International. (2014). Standard test method for compressive strength of cylindrical concrete specimens. *ASTM C39/C39M-14*.
12. ASTM International. (2016). Standard test methods and definitions for mechanical testing of steel products. *ASTM A370-16*.
13. Thamrin, R.; and Kaku, T. (2005). Tension force model of longitudinal reinforcement at the support of RC beam with hanging region. *Proceedings of FIB Symposium on Keep Concrete Attractive"*. Budapest, 613-618.
14. Thamrin, R.; and Kaku, T. (2007). Bond behavior of CFRP bars in simply supported reinforced concrete beam with hanging region. *Journal of Composites for Construction, ASCE*, 11(2), 129-137.
15. ACI Committee 318. (2014). Building code requirements for structural concrete (ACI 318M-14) and commentary on building code requirements for structural concrete (ACI 318RM-14). *ACI Standard and Report*.
16. Park, R.; and Paulay, T. (1975). *Reinforced concrete structures*. New York: John Wiley.
17. Mander, J.B.; Priestley, M.J.N.; and Park, R. (1988). Theoretical stress-strain model for confined concrete. *Journal of Structural Engineering*, 114(8), 1804-1826.